

# We are IntechOpen, the world's leading publisher of Open Access books Built by scientists, for scientists

6,900

Open access books available

186,000

International authors and editors

200M

Downloads

Our authors are among the

154

Countries delivered to

TOP 1%

most cited scientists

12.2%

Contributors from top 500 universities



WEB OF SCIENCE™

Selection of our books indexed in the Book Citation Index  
in Web of Science™ Core Collection (BKCI)

Interested in publishing with us?  
Contact [book.department@intechopen.com](mailto:book.department@intechopen.com)

Numbers displayed above are based on latest data collected.  
For more information visit [www.intechopen.com](http://www.intechopen.com)



# Cloud Microorganisms, an Interesting Source of Biosurfactants

*Pascal Renard, Isabelle Canet, Martine Sancelme,  
Maria Matulova, Iveta Uhliarikova, Boris Eyheraguibel,  
Lionel Nauton, Julien Devemy, Mounir Traïkia,  
Patrice Malfreyt and Anne-Marie Delort*

## Abstract

A new scientific hypothesis states that biosurfactants from cloud microorganism origin could change the surface tension of aerosols and thus the mode of precipitations. In order to check this hypothesis, our team has screened a collection of 480 microbial strains isolated from cloud waters for the production of biosurfactants and showed that 42% of these strains were producing such molecules. In the present work, we isolated and identified by LC-MS-MS lipopeptides produced from three strains issued from this screening. Viscosin and massetolide E (cyclic lipopeptides) were produced by *Pseudomonas* sp. PDD-14b-2, and syringafactins (linear lipopeptides) were produced by *Xanthomonas campestris* PDD-32b-52 and *Pseudomonas syringae* PDD-32b-74. The critical micelle concentration (CMC) of these biosurfactants was determined using the pendant drop method. Finally, two approaches of molecular dynamics were used to model the conformation of viscosin and syringafactin A at the water-air interface: one is based on all-atoms simulation (CHARMM force field), while the other one on coarse-grain (CG) simulation (MARTINI force field). To conclude, this work shows how the biodiversity of the cloud microbiota can be explored to search and produce biosurfactants of interest both for atmospheric sciences and also for biotechnological applications.

**Keywords:** cloud, mass spectrometry, biosurfactants, lipopeptides, *Pseudomonas*, *Xanthomonas*, modeling

## 1. Introduction

The structure and function of microbial communities in clouds have been studied only very recently. Although clouds are hostile environments (with acidic pH, low temperature, UV exposure, and oxidative medium), it was shown that microorganisms are alive and metabolically active [1, 2]. Our team was pioneer in isolating and describing microbial strains in cloud water isolated at the summit of the Puy de Dôme mountain, which is referenced as a European site for cloud studies [3–5]. Long-term survey at this site allowed to evaluate concentrations of  $10^5$  bacteria  $\text{mL}^{-1}$  and  $10^4$  fungi and yeasts  $\text{mL}^{-1}$  of cloud water. The most frequently encountered

genera of cultivable bacteria are *Pseudomonas*, *Sphingomonas*, *Streptomyces*, *Rhodococcus*, and *Bacillus*, while *Dioszegia*, *Udeniomyces*, and *Cryptococcus* are dominant genera for cultivable yeasts [5]. Metagenomics and other DNA-based analyses confirmed the predominance of Proteobacteria, Actinobacteria, and Firmicutes [2, 6]. Recent metatranscriptomics data showed that Proteobacteria are the most active in clouds [6].

Microorganisms have long been considered as inert particles traveling in the atmosphere; however, the discovery of their metabolic activity suggested they could play a role in atmospheric chemistry and in the microphysics of clouds [1, 2, 7].

Concerning atmospheric microphysics, one of the most difficult scientific problems today is to improve the fundamental understanding and prediction of cloud formation in the atmosphere. Recent papers have highlighted the role of surfactants in atmospheric particles, a role predicted by theory 80 years ago but denied by the scientific community for decades [8, 9]. The group of Barbara Nozière extracted organic compounds from atmospheric aerosols that were able to lower the surface tension ( $\sigma$ ) under  $30 \text{ mN}\cdot\text{m}^{-1}$  for concentrations 5 or 6 orders of magnitude lower than those for organic acids [10–14].

These very low values suggested the presence of biosurfactants, and these surface-active agents are of microbial origin and are extremely efficient compared to classical surfactants [15–17]. They are amphiphilic with a lipid tail (hydrophobic) and a sugar or peptide moiety (hydrophilic). Although their chemical composition is extremely diverse, they can be classified in two main categories based on their molecular mass [15, 18, 19]: (1) small biosurfactants (PM < 1000 amu) including glycolipids (rhamnolipids, trehalolipids, sophorolipids etc.) and lipopeptides (viscosin, surfactin, polymyxin, syringomycin etc.) and (2) polymeric structures (PM  $10^6$  amu) such as polysaccharides, proteins, liposaccharides, lipoproteins (alasan, emulsan etc.).

Biosurfactants could affect atmospheric microphysics by modifying cloud condensation nuclei (CCN) activation. Owing to their exceptional scope in reducing surface tension, these surface-active compounds are thus likely to enhance the propensity of the aerosols to form clouds, as the activation of particles into cloud droplets depends on surface tension according to Köhler's theory [20].

The discovery of the presence of biosurfactants on aerosols raised a new scientific hypothesis: could these biosurfactants be produced by airborne microorganisms? Traditionally, biosurfactant-producing microorganisms were mainly isolated in environments such as soils, seawaters, and sediments contaminated or not by petroleum products [21–24]. Biosurfactants producers can also be isolated from natural sources including fruits, leaves, honey, sugarcane, insects, marine sponges etc. [24]. More recently, extreme environments were described as sources of biosurfactants, microbial producers were isolated from desert and arid soils or from the cryosphere (polar soils and lakes) [24, 25]. The first report concerning the atmospheric environment was made by Ahern [26]. This team showed that 70 fluorescent *Pseudomonas* strains isolated from cloud and rain waters in Scotland were producing biosurfactants; among them, 43 isolates were high producers. More recently, our group screened 480 microbial strains isolated from cloud water collected at the Puy de Dôme station [27]. This microbial collection was composed mainly of Gammaproteobacteria (23.3%), with a majority of *Pseudomonas*; Alphaproteobacteria (19.8%), with a majority of *Sphingomonas*; Actinobacteria (24.2%); and Basidiomycota (19.6%). Using the pending drop method, we measured the decrease of the surface tension of water droplets (12  $\mu\text{L}$  in volume) induced by the addition of crude culture medium of the different strains. Up to 41% of the tested strains were producing biosurfactants ( $\sigma \leq 55 \text{ mN}\cdot\text{m}^{-1}$ ), 7% of them (*Pseudomonas* and *Xanthomonas* strains) were very active producers ( $\sigma \leq 30 \text{ mN}\cdot\text{m}^{-1}$ ).

These results show that the biodiversity present in clouds and rain can be a very interesting, still unexplored, source of biosurfactants. As atmospheric environments are cold habitats, these results confirm that cold-adapted organisms are good candidates to produce biosurfactants [25].

Biosurfactants may constitute very valuable compounds of industrial interest as they are promising substitutes for synthetic surfactants with higher biodegradability and lower toxicity. They reach such low surface tensions, even for trace concentrations. Typical desirable properties include solubility enhancement, surface tension reduction, and low critical micelle concentrations, higher foaming, higher selectivity, and specific gravity at extreme temperature, pH, and salinity. In terms of economics, biosurfactants can be synthesized from a renewable stock; however, large-scale production remains challenging [28, 29]. The enormous diversity of biosurfactants also makes them an interesting group of materials for application in many areas such as agriculture, public health, food, health care, medicine, cleaning, textiles, nanotechnologies, waste utilization, and environmental pollution control such as in degradation of hydrocarbons present in soil or extraction of heavy metals [15, 16, 18, 19, 28, 30–35].

Considering the potential industrial interest of biosurfactants, we decided to go further in investigating our unique collection of microbial strains isolated from clouds as a source of biosurfactants. The objective of this work was thus to isolate biosurfactants produced by some of the best producers as determined from our previous screening in order to study their structure and their critical micelle concentration (CMC) properties. In addition, we were interested in modeling their conformation at the water-air interface to understand better their behavior in making cloud droplets. To reach these goals, we selected three strains isolated from clouds (*Pseudomonas* sp. PDD-14b-2, *Xanthomonas campestris* PDD-32b-52, and *Pseudomonas syringae* PDD-32b-74) that were high biosurfactant producers [27].

## 2. Materials and methods

### 2.1 Production and purification of biosurfactants

*Pseudomonas* sp. PDD-14b-2 (GenBank accession number of the 16S rRNA gene sequence: DQ512788), *Xanthomonas campestris* PDD-32b-52 (HQ256850), and *Pseudomonas syringae* PDD-32b-74 (HQ256872) were isolated from cloud water sampled at the Puy de Dôme summit (1465 m) [5]. The isolates obtained in pure cultures (R2A, 17°C) were stored in 10% (v/v) glycerol at –80°C.

For each strain, preculture was performed from the glycerol stocks in 100 mL of a R2A growth medium [36] at 17°C. After 3 days, the inoculum was grown in 10 Erlenmeyer flasks containing 200 mL of R2A medium (2% v/v plating). Cultures were incubated at 17°C at 200 rpm. The growth was monitored through measurement of optical density and pH, the production of biosurfactants by measurement of the surface tension of the supernatant. After 3–5 days, cultures were centrifuged (8000 rpm) at 4°C for 15 min. Supernatants were combined (1.8 L) and pH adjusted to 6.1.

Concentration of biosurfactants was achieved using a chromatographic method initially described by Reiling [37] for rhamnolipids, through adsorption chromatography on an Amberlite XAD2 (Sigma-Aldrich) column [38]. After equilibration to pH 6.1 using 0.1 M phosphate buffer, supernatant was passed through the resin (300 mL.h<sup>-1</sup> outflow) until saturation of the resin occurred (monitored by measuring the surface tension of the column outlet). The column was then washed by three volumes of distilled water before eluting the biosurfactants with three volumes of methanol. The process is repeated until complete treatment of the supernatant. Methanol fractions are collected and evaporated to dryness using a rotary evaporator.

Purification was then undergone by flash chromatography (puriFlash®) on a Chromabond® C18 column. Gradient elution was applied (water (A), acetonitrile (B), 5–95% B in 30 min.). Fractions (25 mL) were collected at a flow rate of 12.5 mL per minute over a period of 40 min. UV-detection of biosurfactants was made simultaneously at 219 and 237 nm.

## 2.2 Structure identification by LC-MS/MS

Identification of biosurfactants was performed using an ultra-high-resolution mass spectrometer (LTQ-Orbitrap™, Thermo Scientific) coupled to an electrospray ionization (ESI) source.

Samples were directly infused into the ESI source. The mobile phases consisted in (A) 0.1% formic acid in water (Fluka, 98%) and (B) acetonitrile (CAN; Optima LC-MS, Fischer). The gradient elution was performed at a flow rate of 5  $\mu\text{L min}^{-1}$  using 5–95% of B within 11 min. The sample injection volume was 10  $\mu\text{L}$ . Each sample was measured in the negative and positive ionization modes, with the following optimized settings: source voltage 4 kV and capillary temperature 350°C, in the positive mode. Transient acquisition time was set to 1 s, which corresponds to a nominal resolution of 3 ppm, and to observe individual peaks resolution (FWHM) typically better than 70,000 ( $m/z$  200). Identification was performed using MS/MS fragmentation to confirm the structure of the products. MS/MS experiments were carried out with a collision energy of 5 eV.

Data were collected from  $m/z$  50 to 1200 in the positive and negative ionization modes. Elemental compositions from exact mass measurement were assigned using Xcalibur® software (Thermo Scientific). The data processing was done through the following steps: (1) the assignment of  $m/z$  for each spectrum signal, (2) internal calibration of spectrum by homologs biosurfactant using the most intense class, (3) assignment of molecular formula for each signal by comparing experimental  $m/z$  with a theoretical  $m/z$  database for possible biosurfactant, and (5) solving of dubieties on molecular formula assignments by confirming the isotopic ratio.

## 2.3 Surface tension measurements

Samples were centrifuged (10,480 g/3 min) just prior to surface tension measurements. All surface tension measurements were performed using the pendant drop method with an OCA 15 Pro tensiometer (Data Physics, Germany). The camera analyzes the pendant drop profile of the crude extract. A dosing needle with a 1.65-mm outside diameter was used, producing drops of 12  $\mu\text{L}$ . The software fits this latter measurement to the Young-Laplace equation and averages out surface tension from all measurements [39]. The measurements were obtained at 295 K every second. The tensiometer was calibrated using Milli-Q water. The uncertainty of the instrument was  $\pm 0.01 \text{ mN}\cdot\text{m}^{-1}$ . Each dynamic surface tension curve was measured three times for the most efficient biosurfactant-producing microorganisms, and the measurements displayed  $\pm 10\%$  variation. These dynamic surface tension measurements lasted until the equilibrium region was reached (maximum 30 min [27]). Along with the surface tension, each measurement also provided real-time monitoring of the droplet volume, facilitating an assessment of evaporation. No significant evaporation (<5%) was observed during the experiments [27].

## 2.4 Modeling

Molecular dynamics based on all-atoms simulation was performed using NAMD programs with CUDA gpu acceleration designed especially for large

biomolecular systems. The force field used is CHARMM with CHARMM22 parameter files. All air/water interface models were constructed using VMD as molecular visualization program. The water used in our solvent boxes is TIP3 water. Each model undergoes the same treatment: a first phase of minimization, followed by a canonical dynamics for reaching the set temperature of 298 K, and a second phase of pressure equilibration at 1 atm in isothermal-isobaric ensemble followed by a third phase of production in the same isothermal-isobaric ensemble for a duration of 20 nanoseconds.

The coarse-grain (CG) molecular dynamics were performed by using the MARTINI force field [1, 2] at 300 K in the NVT statistical ensemble. The liquid-vapor interfaces were modeled using a parallelepipedic box of dimensions  $L_x = 60 \text{ \AA}$ ,  $L_y = 60 \text{ \AA}$ , and  $L_z = 570 \text{ \AA}$ . The total number of CG water molecules was fixed to 6000 and the number of surfactants was varied from 4 to 32 for each interface. A CG water molecule corresponds to four water molecules. The equilibration time was set to 110 ns whereas the thermodynamics and structural properties were averaged during the acquisition phase over 200 ns.

### 3. Results and discussion

#### 3.1 Production and purification of biosurfactants

The 3 strains *Pseudomonas sp.* PDD-14b-2, *Xanthomonas campestris* PDD-32b-52, and *Pseudomonas syringae* PDD-32b-74 were selected from the screening of 480 strains isolated from cloud waters for their effectiveness in reducing surface tension [27]. They all belong to the class of Gammaproteobacteria and are representative of a genus very commonly encountered in cloud water samples [5].

For the production of biosurfactants, the bacterial cultures were carried out in R2A medium, a relatively poor but diversified medium in carbon and nitrogen sources, initially developed to isolate microorganisms from tap water. We choose this medium, without supplementing with compounds known to favor the production of biosurfactants, as it is representative of the cloud environment in its composition.

On each culture, the simultaneous kinetic monitoring of the bacterial growth and the decrease of the surface tension, using as reference value that of the medium R2A ( $62\text{--}64 \text{ mN}\cdot\text{m}^{-1}$ ), allowed us to stop the cultures for an optimal production of biosurfactants.

Extraction of the lipopeptides was carried out by adapting an adsorption column chromatography method (using Amberlite) initially described by Reiling [37] for the concentration of rhamnolipids. The surface tension of the crude supernatants was  $25 \text{ mN}\cdot\text{m}^{-1}$ . The adsorption of the biosurfactants was easily monitored by the measurement of the surface tension of the aqueous fractions at the column outlet, and the saturation of the column was detected when the surface tension reached a value greater than  $40 \text{ mN}\cdot\text{m}^{-1}$ . The biosurfactants were then eluted with methanol. One advantage of the technique is that if the entire supernatant cannot be processed at one time, the operation is repeated until it is fully treated. We have thus shown that the use of adsorption column chromatography is particularly suitable for the extraction of lipopeptides. In addition, compared to conventional methods of extraction using organic solvents (preceded or not by acid precipitation) [40], this method effectively eliminates the culture medium nutrients present in the supernatant and leads to a pre-concentration of biosurfactants which then allows easier purification by reversed phase chromatography.

### 3.2 Identification and surfactant properties of viscosin and massetolide E produced by *Pseudomonas sp.* PDD-14b-2

Two biosurfactants issued from the culture of a cloud bacterium *Pseudomonas sp.* PDD-14b-2 were purified using an Amberlite column and a puriFlash® system. The structure of these biosurfactants was identified as that of cyclic lipopeptides (viscosin and massetolide E) using high-resolution LC-MS/MS. **Figure 1A** presents the ESI-MS-MS spectrum of viscosin, the details of the fragmentation of this molecule are shown in **Figure 1B** and **C**.

Viscosin gave a ( $[M + H]^+$ ) protonated molecule at  $m/z$  1126.699 (theoretical  $m/z$  1126.697) appropriate for a molecular formula of  $C_{54}H_{95}N_9O_{16}$  (monoisotopic mass is  $1125.69 \text{ g}\cdot\text{mol}^{-1}$ ).

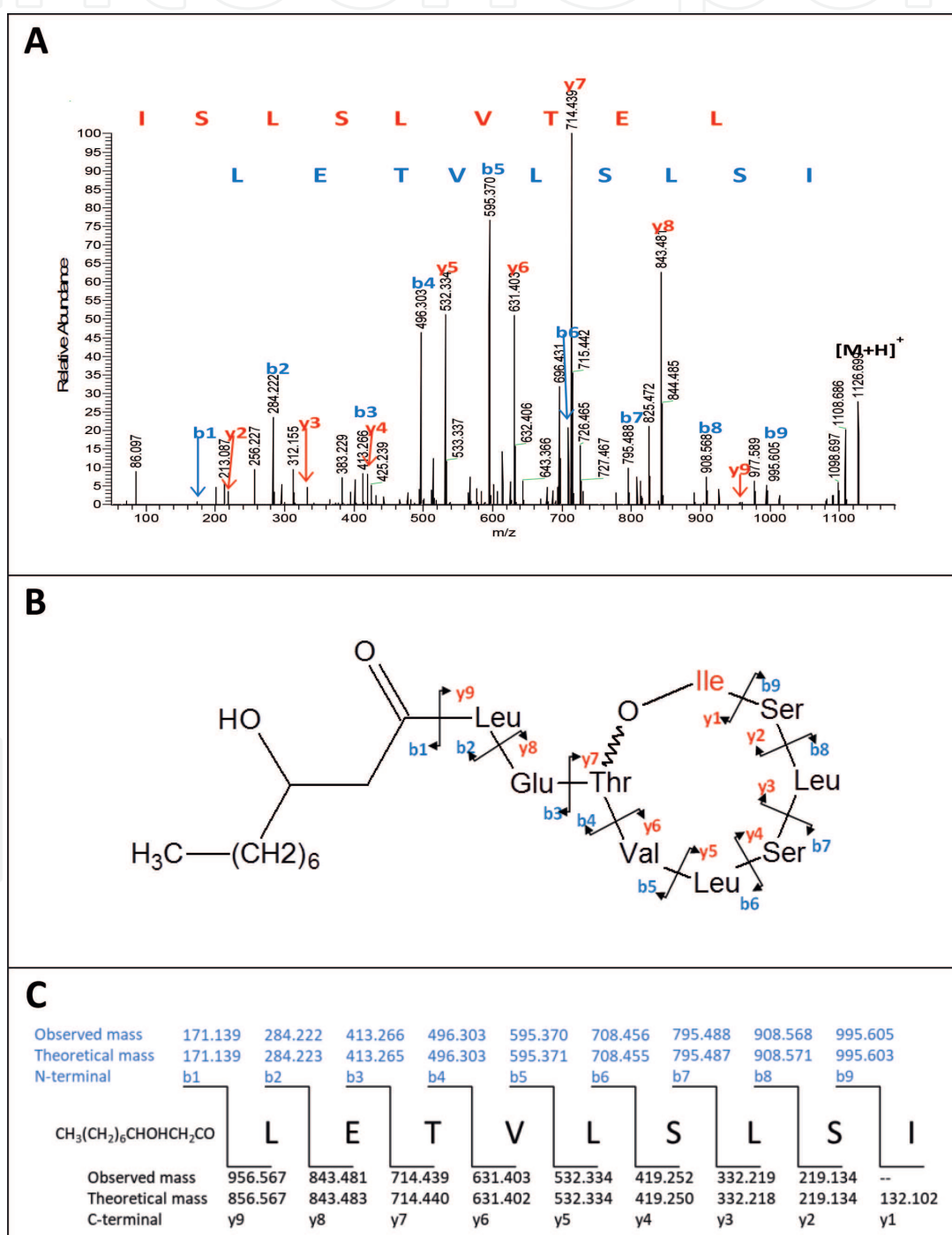


**Figure 1.** (A) ESI-MS/MS (collision-induced dissociation) spectrum of parent ion of viscosin ( $m/z$  1126.699), (B) Chemical structure (fragments) for viscosin, (C) Identification of the fragments of viscosin. The  $Y_1$  fragment could be either isoleucine (I) or leucine (L).

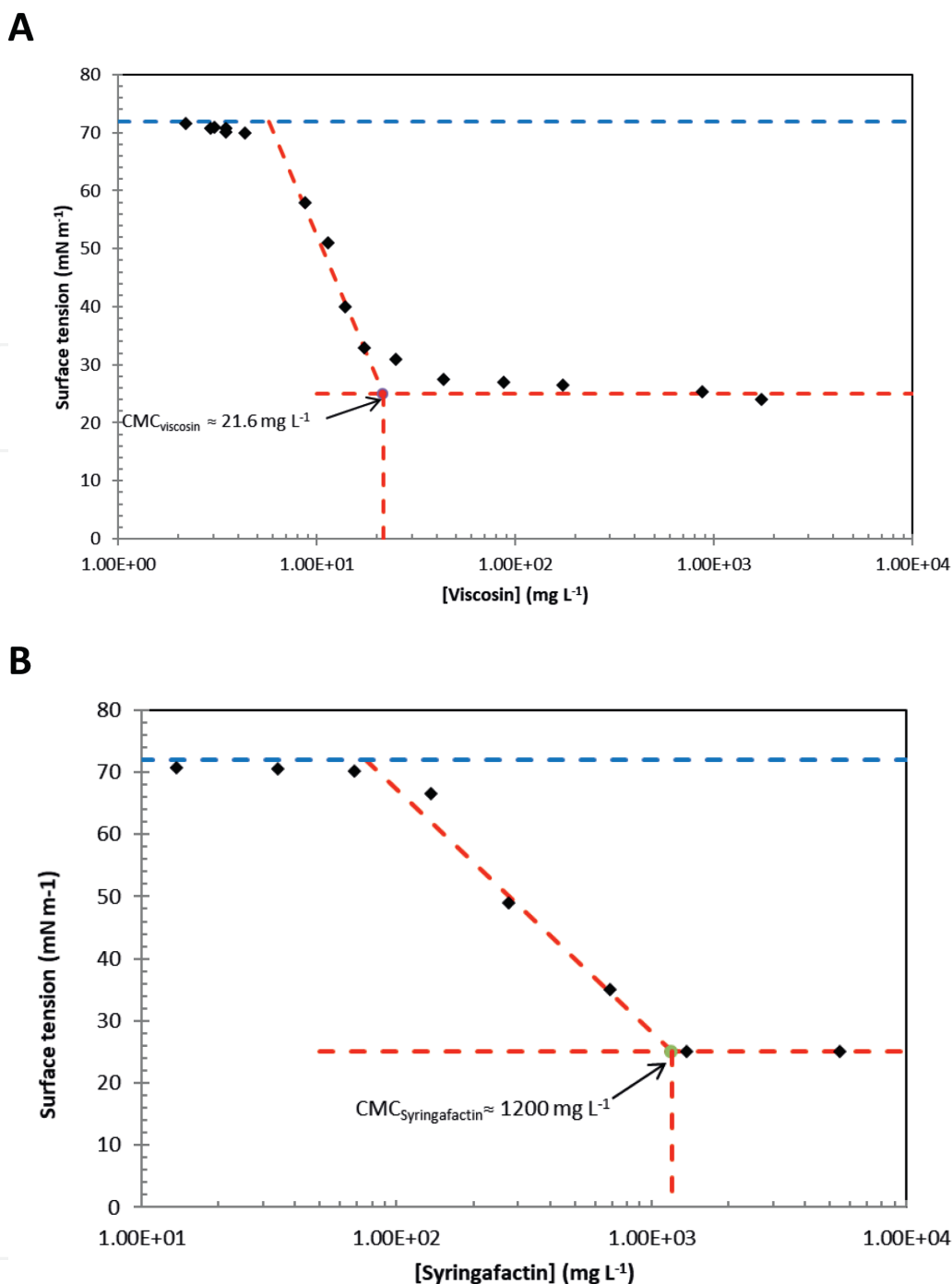


**Figure 2.** Determination of the surface tension curve and CMC value of biosurfactants by the pendant drop technique. The red dot represents the initial crude extracts (consisting of the supernatants of the pure cultures). The black dots at lower concentrations are those obtained from successive dilutions. The blue dashed line represents the value for pure water, and red dashed lines illustrate the graphical determination of the CMC. (A) Viscosin CMC = 25 mN.m<sup>-1</sup> at 21.6 mg.L<sup>-1</sup>; (B) Syringafactin B/C CMC = 25 mN.m<sup>-1</sup> at 1.2 gL<sup>-1</sup>.

In the same way and with the same precision (observed mass: m/z 1112.684; theoretical mass: m/z 1112.682), we identified the massetolide E (C<sub>53</sub>H<sub>93</sub>N<sub>9</sub>O<sub>16</sub>) whose structure is rather similar to that of viscosin, the last amino acid fragment is a valine instead of a leucine.

These high-resolution MS data are consistent with those obtained by Gerard [41] who isolated and identified massetolides A–H and viscosin from two *Pseudomonas* strains isolated from marine environment.

The synthesis of viscosin has been reported by other *Pseudomonas* strains including *P. syringae*, *P. tolaasii*, *P. fuscovaginae*, *P. corrugate*, *P. fluorescens*, *P. libanensis*, and *P. putida* [16, 42–45]. Massetolides whose structures are very closely

related to those of viscosin are less frequently described; massetolide A was produced by *P. fluorescens* SS101 [46].

We measured the surface tension of the isolated viscosin and determined its CMC using the pendant drop method (**Figure 2A**). This CMC is extremely low ( $21.6 \text{ mg.L}^{-1}$  for a minimum surface tension of  $25 \text{ mN.m}^{-1}$ ) showing that this molecule has very strong biosurfactant properties. Very few authors measured the CMC of viscosin; Saini [42] found a value of  $54 \text{ mg.L}^{-1}$  for a minimum surface tension of  $27.5 \text{ mN.m}^{-1}$  for viscosin isolated from *P. libanensis* M9 while de Bruijn [46] measured a CMC of  $10\text{--}15 \text{ mg.L}^{-1}$  for a surface tension around  $30 \text{ mN.m}^{-1}$  for viscosin isolated from *P. fluorescens* SBW25. These CMC values are within the same range of order of our results for the case of *Pseudomonas sp.* PDD-14b-2.

Viscosin is one of the most effective biosurfactants among the cyclic lipopeptides of pseudomonads together with arthrofactin (minimum surface tension of  $24 \text{ mN.m}^{-1}$ , CMC of  $13.5 \text{ mg.L}^{-1}$ ) [45]. In spite of its very low CMC, viscosin has not yet been produced and exploited at an industrial scale. Some studies report viscosin as a surface-active, bioemulsifier with anticancer properties and massetolide as a biocontrol agent [16]. Raaijmakers [22] pointed out natural functions of viscosin and massetolide A including their role in mobility and biofilm formation.

### 3.3 Identification and surfactant properties of syringafactins produced by *Xanthomonas campestris* PDD-32b-52 and by *Pseudomonas syringae* PDD-32b-74

Using the same technique as described before, we produced and purified syringafactins (linear lipopeptides) by cultivation of two strains isolated from clouds (*Xanthomonas campestris* PDD-32b-52 and *Pseudomonas syringae* PDD-32b-74). Their amino acid sequence was identified by LC-MS-MS (**Figure 3**) using the same methodology for fragment assignments as described for viscosin (**Figure 3B and C**). Six types of syringafactins (A, B, C, D, E, and F) could be identified; syringafactins B/C and E/F were isolated as mixtures.

The ESI-MS-MS data obtained in this work and used to assign the syringafactin structures are fully consistent with those initially published by Berti [47]. Syringafactins are the only linear lipopeptides described up to now and are poorly documented. They were first isolated from *P. syringae* pv. tomato DC3000 [47] and more recently from *P. syringae* pv. syringae B728a 5b [48]. We show here that they can be produced by another strain of *Pseudomonas syringae* (*P. syringae* PDD-32b-74) and also by a strain of *Xanthomonas* (*X. campestris* PDD-32b-52).

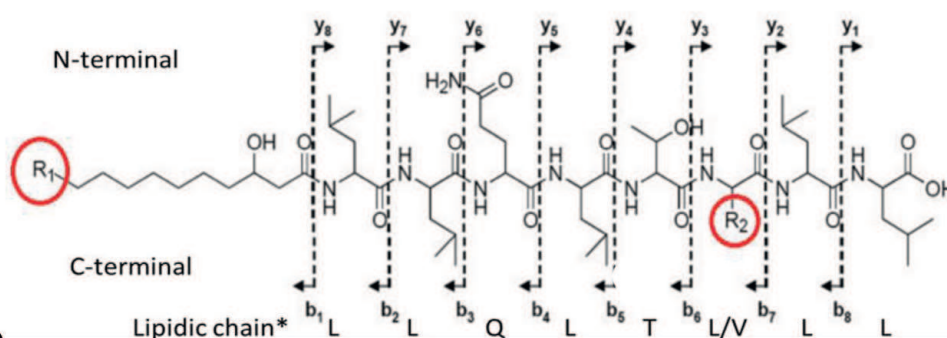
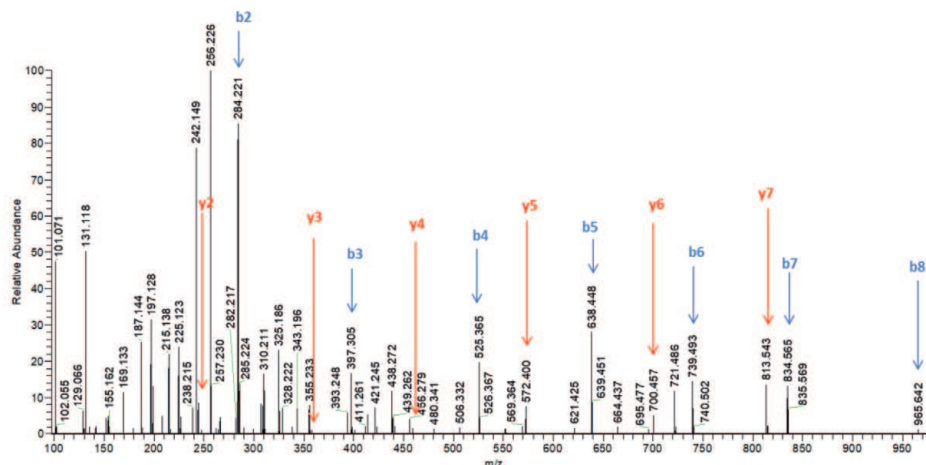
The measured CMC of syringafactin B/C was  $1.2 \text{ g.L}^{-1}$  for a minimum surface tension of  $25 \text{ nM.m}^{-1}$  (**Figure 2B**) proving the surfactant properties of this molecule. To our knowledge, this is the first report of a CMC value for this compound. This CMC is much higher than that of viscosin and closer to that of syringomycin, a cyclic lipopeptide, produced by *Pseudomonas syringae* B301D (CMC of  $1.25 \text{ mg.L}^{-1}$  and minimum surface tension of  $33 \text{ mN.m}^{-1}$ ) [45].

Biotechnological applications of syringafactins are not described yet, only natural functions related to their secretions by *Pseudomonas syringae* isolates present on the phyllosphere are described (enhancement of bacterial fitness on leaf surfaces during fluctuating humidity, swarming motility) [47, 48].

### 3.4 Modeling the conformation of biosurfactants at the water-air interface

Both descriptions can be used to simulate interfacial systems: an atomistic description that performs very well for relatively small and simple systems and a

**A**



**B**

Observed mass	—	284.221	397.305	525.363	638.448	739.496	834.565*	965.642	
Theoretical mass	171.139	284.223	397.307	525.366	638.450	739.498	852.582	965.666	
N-terminal	b1	b2	b3	b4	b5	b6	b7	b8	
	$R_1(CH_2)_7CHOHCH_2CO$	L	L	Q	L	T	$R_2$	L	L
Observed mass		843.481	714.439	631.403	532.334	419.252	332.219	219.134	--
Theoretical mass		926.629	813.545	700.461	572.402	459.318	358.270	245.186	132.102
C-terminal		y8	y7	y6	y5	y4	y3	y2	y1

**C**

**D**

<b>Syringafactin A</b>	<b>(R1: H / R2: Val)</b>	<b>C<sub>54</sub>H<sub>99</sub>O<sub>13</sub>N<sub>9</sub></b>	<b>1081.736 amu</b>
<b>Syringafactin B/C</b>	<b>(R1: H / R2: Leu)</b>	<b>C<sub>55</sub>H<sub>101</sub>O<sub>13</sub>N<sub>9</sub></b>	<b>1095.752 amu</b>
<b>Syringafactin D</b>	<b>(R1: CH<sub>3</sub>CH<sub>2</sub> / R2: Val)</b>	<b>C<sub>56</sub>H<sub>103</sub>O<sub>13</sub>N<sub>9</sub></b>	<b>1109.768 amu</b>
<b>Syringafactin E/F</b>	<b>(R1: CH<sub>3</sub>CH<sub>2</sub> / R2: Val)</b>	<b>C<sub>57</sub>H<sub>105</sub>O<sub>13</sub>N<sub>9</sub></b>	<b>1123.783 amu</b>

**Figure 3.**

(A) ESI-MS/MS (collision-induced dissociation) spectrum of parent ion of syringafactin B/C ( $m/z$  1095.752), (B) Chemical structure (Fragments) for syringafactin, (C) MS/MS fragmentation for the syringafactin B/C with  $R_1$ : H and  $R_2$ : Leu (b7 fragment is dehydrated), (D) Formula and exact masses of the different syringafactins.

CG model that is designed for complex interfacial systems involving surfactants for example. Nevertheless, these two descriptions may even be complementary. Indeed, the CG model can be built from the configurations obtained at the atomistic level through a bottom-up approach.

**Figure 4A** shows the structure of viscosin at the water-air interface with the distribution of the hydrophobic and hydrophilic zones. **Figure 4B** presents the density

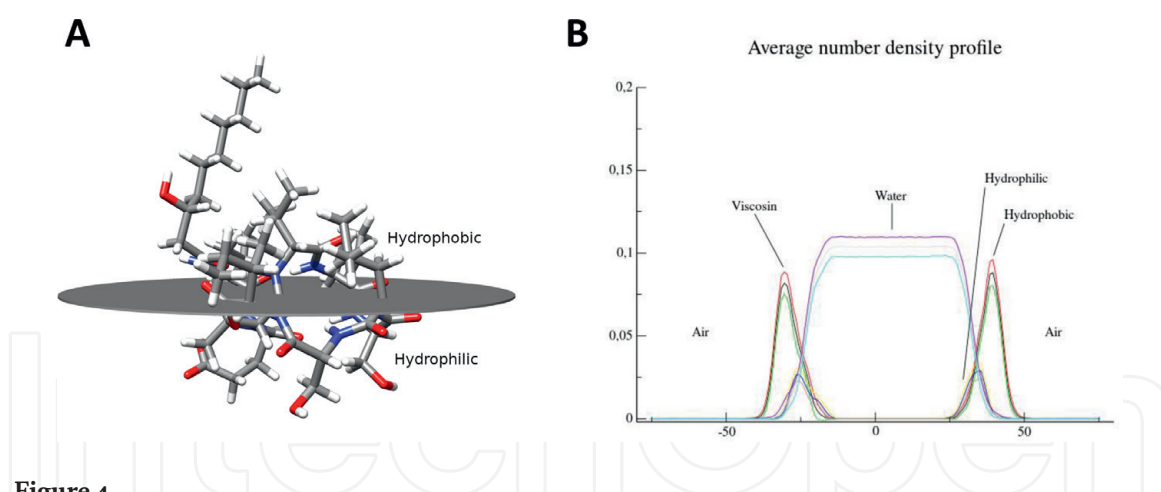


**Figure 4.** (A) Structure of viscosin. (B) Viscosin at the water-air interface in a water box using all-atoms simulation (CHARMM force field).

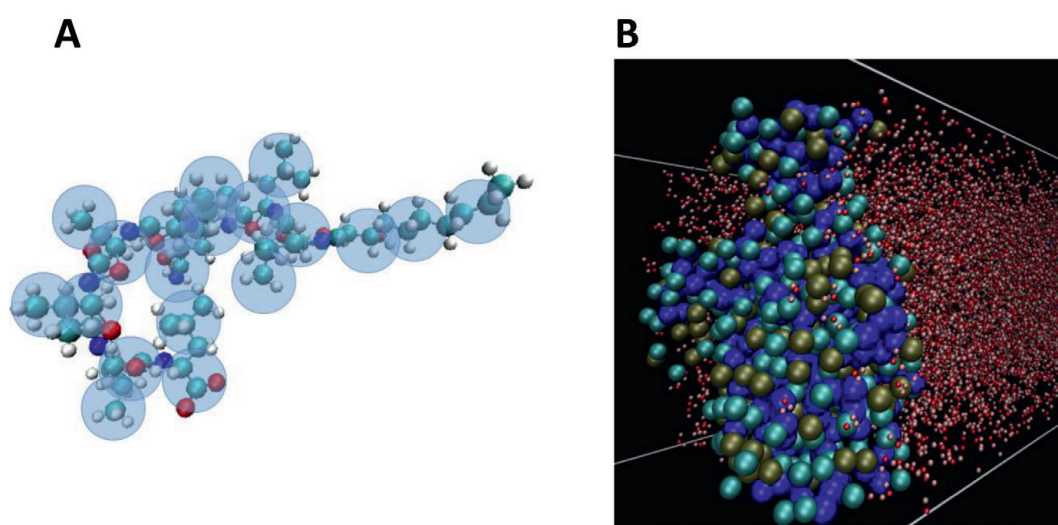


**Figure 5.** (A) CG structure of syringafactin A represented. (B) Typical configuration of a liquid-vapor water interface with 32 surfactants at each interface.

profiles of the water box containing viscosin. These profiles were obtained by running a trajectory over 20 ns and establish a bidimensional structure of the biosurfactant at the water-air interface. The hydrophobic parts defined by the leucine (L); valine (V); isoleucine (I); and alanine, cysteine and glycine (ACG) amino acids of the surfactant populate the side of the interfacial region toward the vapor phase. The hydrophilic parts defined by the group of glutamic acid (E) and serine (S) amino acids are rather located at the interface at the position of the Gibbs dividing plane. The density profiles have been calculated by using atomistic models with 30 surfactant molecules at each interface. We also show that the liquid-water region is quite well developed over a region of 40 Å. This is a necessary condition to simulate the behavior of surfactants at least at the atomistic level.

These atomistic simulations take a very long time to equilibrate the interfacial region.

It is well known that the use atomistic force field models is problematic for simulating complex liquid-vapor interfacial systems with surfactants that relax over time and length scales inaccessible for these atomistic descriptions. An alternative is to simplify the model by using a CG description [49, 50] for which the key element called a bead represents several atoms or molecules. By using these CG models [51–53], we can improve the description of the systems by using larger system sizes. The modeling of the interfacial systems with surfactants can then be conducted by CG models [51–53]. **Figure 5A** shows the CG representation of syringafactin A and

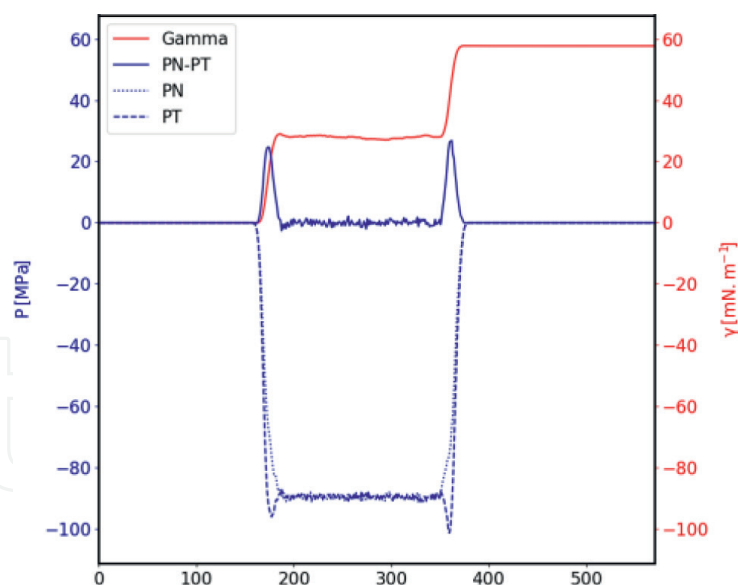


**Figure 6.** Profiles of the normal  $P_N(z)$  (MPa) and tangential  $P_T(z)$  (MPa) components of the pressure tensor, the difference  $(P_N(z) - P_T(z))$  (left axis) and the integral  $\gamma(z)$  (right axis) as a function of the  $z$ -axis (direction normal to the interface). These profiles are calculated in the liquid-vapor interface of water with four surfactants at each interface.

**Figure 5B** represents an equilibrated liquid-vapor water interface with 32 biosurfactants in the interfacial region.

One of the key properties in the modeling of the liquid-vapor systems is the interfacial tension. It is now well known that the calculation of this property is under control at the atomistic level [54–57]. It is far from being the same for the CG simulations. Indeed, an accurate calculation of the interfacial tension requires to check that the mechanical equilibrium of the CG liquid-vapor equilibrium is respected. **Figure 6** shows the profiles of the normal ( $P_N$ ) and tangential ( $P_T$ ) components of the pressure tensor along the direction normal to the interface calculated in the liquid-vapor interface of water with four surfactants at each interface. The profile of the difference ( $P_N - P_T$ ) exhibits two peaks at both interfaces and no contribution in the water bulk liquid and vapor phases.  $\gamma(z) = \frac{1}{2} \int_0^{L_z} (P_N(z) - P_T(z)) dz$  is the local interfacial tension along the direction normal to the interface. As expected from mechanical equilibrium and observed in **Figure 6** (blue curve), this profile is flat in the bulk phases with two symmetric contributions at both interfaces. The resulting interfacial tension is about  $60 \text{ mN.m}^{-1}$  and does not deviate very much from experiments. Whereas the prediction of the surface tension, calculated from atomistic simulations, is quantitative, it is still subject to some adjustments due to the CG nature of the interactions. It means that the CG model must be calibrated on this property to predict in the future both the interfacial tension and its dependence on the concentration of surfactants [51]. Indeed, recent studies [52, 53] show that the degree of coarse-graining impacts on the description of the interface. A good reproduction of the interfacial tension requires a new parametrization of the CG model by considering the interfacial tension in the experimental database.

Nevertheless, the use of CG models has the advantage of providing very well-equilibrated interfacial regions. **Figure 7** shows the density profiles along the  $z$ -axis for the liquid-vapor interface of water with both 4 and 32 syringafactin molecules at each interface. We observe that the surfactant molecules populate the interfaces with sharp peaks at weak concentrations (**Figure 7a**). At strong concentrations, we observe that the thickness of the interface increases. In any case, the interfacial region is well recovered by surfactants with no preferential coverage between the lipid and protein parts of the syringafactin molecule. We only observe a slight increase of coverage of the lipid part on the vapor side.

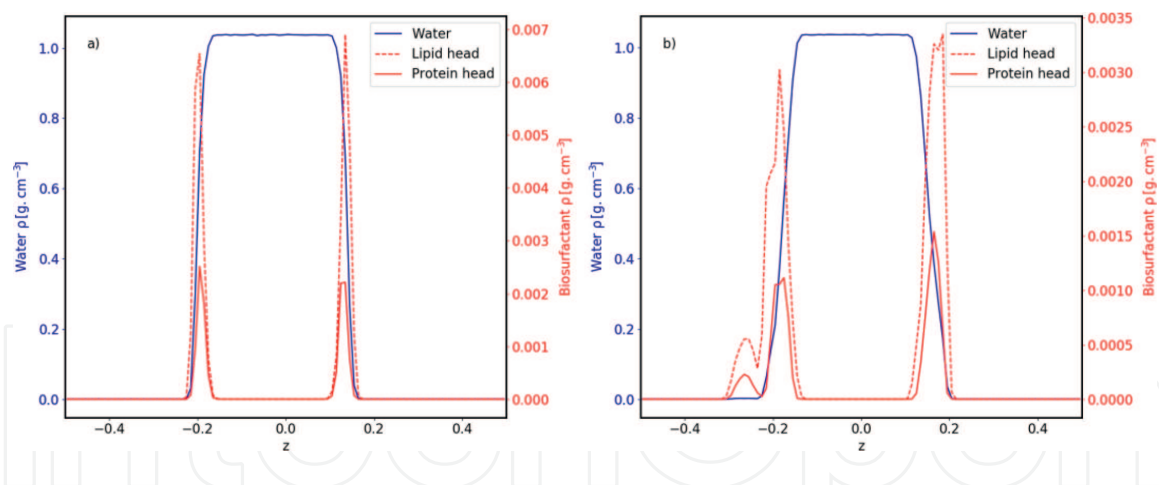


**Figure 7.**

Density distributions of the water and different parts of the syringafactin molecules at two surfactant concentrations: (a) 4 surfactant molecules and (b) 32 surfactant molecules at each interface. The lipid head is represented by the first three beads of the lipid chain whereas the protein part is represented by a typical bead of this part.

On this aspect of modeling complex interfacial systems, we can conclude that the development of CG models will open the way to new force fields capable of quantitatively predicting the surface tension and main properties such as the CMC. The prediction of the CMC, already operational for some CG models [51], will require additional adjustments for new molecules with various intramolecular interactions. The development of CG force fields using mesoscale simulation methods [58–60] is an active area of research. Different methodologies coexist to develop these CG interactions: a bottom-up approach consisting in deriving the force field from atomistic simulations and a top-down approach aiming to build the parameters of the model from mapping onto macroscopic properties such as the interfacial tension.

## 4. Conclusions

This work is the first report of a detailed study of biosurfactants produced by *Pseudomonas* and *Xanthomonas* strains isolated from cloud samples. We have used a convenient method to purify these compounds based on adsorption on Amberlite coupled with a puriFlash® chromatographic technique; the different steps were monitored using the pendant drop method. High-resolution LC-MS-MS allowed assigning unambiguously the structure of viscosin, massetolide E, and different syringafactins. The measurements of CMC of viscosin and syringafactin showed that viscosin is a particularly powerful biosurfactant. Finally, two approaches of molecular dynamics were used to model the conformation of these biosurfactants at the water-air interface: an atomistic description for viscosin (CHARMM force field) and a CG model for syringafactin A (MARTINI force field). This last approach is particularly original and promising. To our knowledge, these studies constitute the first modeling of interfacial properties of such complex biosurfactants.

In addition to fundamental knowledge of biosurfactant properties, this work shows that cloud microorganisms can provide an unexplored source of biosurfactants. Rather few strains, mainly *Pseudomonas*, were shown to produce viscosin, massetolides, and syringafactins, and two new isolates from this genus are described here. We report here the first production of syringafactins by a strain of *Xanthomonas*. Considering that more than 30 strains of our microbial collection isolated from clouds were very active biosurfactant producers ( $\sigma \leq 30 \text{ mN.m}^{-1}$ ) [27], further investigation is very promising to isolate and study other unusual or even new biosurfactants.

## Acknowledgements

This work was funded by the French-USA program ANR-NSF SONATA and the French-Slovak Program Stefanik N° 35588ZE.

## Conflict of interest

The authors declare no conflict of interest.

## Author details

Pascal Renard<sup>1</sup>, Isabelle Canet<sup>1</sup>, Martine Sancelme<sup>1</sup>, Maria Matulova<sup>2</sup>,  
Iveta Uhliarikova<sup>2</sup>, Boris Eyheraguibel<sup>1</sup>, Lionel Nauton<sup>1</sup>, Julien Devemy<sup>1</sup>,  
Mounir Traïkia<sup>1</sup>, Patrice Malfreyt<sup>1</sup> and Anne-Marie Delort<sup>1\*</sup>

<sup>1</sup> Université Clermont Auvergne, CNRS, Sigma-Clermont, Institut de Chimie de  
Clermont-Ferrand, Clermont-Ferrand, France

<sup>2</sup> Slovak Academy of Sciences, Bratislava, Slovakia

\*Address all correspondence to: [a-marie.delort@uca.fr](mailto:a-marie.delort@uca.fr)

## IntechOpen

© 2019 The Author(s). Licensee IntechOpen. This chapter is distributed under the terms of the Creative Commons Attribution License (<http://creativecommons.org/licenses/by/3.0>), which permits unrestricted use, distribution, and reproduction in any medium, provided the original work is properly cited. 

## References

- [1] Delort A-M, Vaïtilingom M, Amato P, Sancelme M, Parazols M, Mailhot G, et al. A short overview of the microbial population in clouds: Potential roles in atmospheric chemistry and nucleation processes. *Atmospheric Research*. 2010;**98**(2):249-260
- [2] Hu W, Niu H, Murata K, Wu Z, Hu M, Kojima T, et al. Bacteria in atmospheric waters: Detection, characteristics and implications. *Atmospheric Environment*. 2018;**179**:201-221
- [3] Amato P, Ménager M, Sancelme M, Laj P, Mailhot G, Delort A-M. Microbial population in cloud water at the Puy de Dôme: Implications for the chemistry of clouds. *Atmospheric Environment*. 2005;**39**(22):4143-4153
- [4] Amato P, Parazols M, Sancelme M, Laj P, Mailhot G, Delort A-M. Microorganisms isolated from the water phase of tropospheric clouds at the Puy de Dôme: Major groups and growth abilities at low temperatures. *FEMS Microbiology Ecology*. 2007;**59**(2):242-254
- [5] Vaïtilingom M, Attard E, Gaiani N, Sancelme M, Deguillaume L, Flossmann AI, et al. Long-term features of cloud microbiology at the puy de Dôme (France). *Atmospheric Environment*. 2012;**56**:88-100
- [6] Amato P, Joly M, Besaury L, Oudart A, Taib N, Moné AI, et al. Active microorganisms thrive among extremely diverse communities in cloud water. *PLoS One*. 2017;**12**(8):e0182869
- [7] Ariya PA, Amyot M. New directions: The role of bioaerosols in atmospheric chemistry and physics. *Atmospheric Environment*. 2004;**38**:1231-1232
- [8] Ruehl CR, Davies JF, Wilson KR. An interfacial mechanism for cloud droplet formation on organic aerosols. *Science*. 2016;**351**(6280):1447
- [9] Noziere B. Don't forget the surface. *Science*. 2016;**351**(6280):1396
- [10] Ekström S, Nozière B, Hultberg M, Alsberg T, Magnér J, Nilsson ED, et al. A possible role of ground-based microorganisms on cloud formation in the atmosphere. *Biogeosciences*. 2010;**7**(1):387-394
- [11] Baduel C, Nozière B, Jaffrezo J-L. Summer/winter variability of the surfactants in aerosols from Grenoble, France. *Atmospheric Environment*. 2012;**47**:413-420
- [12] Noziere B, Baduel C, Jaffrezo J. Dynamic surface tension of atmospheric aerosol surfactants: A new look at cloud activation. *AGU Fall Meeting Abstract*. 2013;**31**:A31D-0110
- [13] Nozière B, Gérard V, Baduel C, Ferronato C. Extraction and characterization of surfactants from atmospheric aerosols. *Journal of Visualized Experiments*. 2017;(122). <https://www.ncbi.nlm.nih.gov/pmc/articles/PMC5565068/>
- [14] Gérard V, Nozière B, Baduel C, Fine L, Frossard AA, Cohen RC. Anionic, cationic, and nonionic surfactants in atmospheric aerosols from the Baltic Coast at Askö, Sweden: Implications for cloud droplet activation. *Environmental Science & Technology*. 2016;**50**(6):2974-2982
- [15] Gautam KK, Tyagi VK. Microbial surfactants: A review. *Journal of Oleo Science*. 2006;**55**(4):155-166
- [16] Mnif I, Ghribi D. Review lipopeptides biosurfactants: Mean classes and new insights for industrial, biomedical, and environmental applications: Lipopeptides Biosurfactants and their Applications. *Biopolymers*. 2015;**104**(3):129-147

- [17] Banat IM, Franzetti A, Gandolfi I, Bestetti G, Martinotti MG, Fracchia L, et al. Microbial biosurfactants production, applications and future potential. *Applied Microbiology and Biotechnology*. 2010;**87**(2):427-444
- [18] Rosenberg E, Ron EZ. High- and low-molecular-mass microbial surfactants. *Applied Microbiology and Biotechnology*. 1999;**52**(2):154-162
- [19] Santos DKF, Rufino RD, Luna JM, Santos VA, Sarubbo LA. Biosurfactants: Multifunctional biomolecules of the 21st century. *International Journal of Molecular Sciences*. 2016;**17**(3):401
- [20] Köhler H. The nucleus in and the growth of hygroscopic droplets. *Transactions of the Faraday Society*. 1936;**32**:1152
- [21] Bodour AA, Drees KP, Maier RM. Distribution of biosurfactant-producing bacteria in undisturbed and contaminated arid Southwestern soils. *Applied and Environmental Microbiology*. 2003;**69**(6):3280-3287
- [22] Raaijmakers JM, De Bruijn I, Nybroe O, Ongena M. Natural functions of lipopeptides from *Bacillus* and *Pseudomonas*: More than surfactants and antibiotics. *FEMS Microbiology Reviews*. 2010;**34**(6):1037-1062
- [23] Jackson SA, Borchert E, O'Gara F, Dobson AD. Metagenomics for the discovery of novel biosurfactants of environmental interest from marine ecosystems. *Current Opinion in Biotechnology*. 2015;**33**:176-182
- [24] Pessôa MG, Vespermann KAC, Paulino BN, Barcelos MCS, Pastore GM, Molina G. Newly isolated microorganisms with potential application in biotechnology. *Biotechnology Advances*. 2019;**37**(2):319-339
- [25] Perfumo A, Banat IM, Marchant R. Going green and cold: Biosurfactants from low-temperature environments to biotechnology applications. *Trends in Biotechnology*. 2018;**36**(3):277-289
- [26] Ahern HE, Walsh KA, Hill TCJ, Moffett BF. Fluorescent pseudomonads isolated from Hebridean cloud and rain water produce biosurfactants but do not cause ice nucleation. *Biogeosciences*. 2007;**4**(1):115-124
- [27] Renard P, Canet I, Sancelme M, Wirgot N, Deguillaume L, Delort A-M. Screening of cloud microorganisms isolated at the Puy de Dôme (France) station for the production of biosurfactants. *Atmospheric Chemistry and Physics*. 2016;**16**(18):12347-12358
- [28] Desai JD, Banat IM. Microbial production of surfactants and their commercial potential. *Microbiology and Molecular Biology Reviews*. 1997;**61**(1):47-64
- [29] Banat IM, Satpute SK, Cameotra SS, Patil R, Nyayanit NV. Cost effective technologies and renewable substrates for biosurfactants' production. *Frontiers in Microbiology*. 2014;**5**. Disponible sur: <https://www.frontiersin.org/articles/10.3389/fmicb.2014.00697/full>
- [30] Lang S. Biological amphiphiles (microbial biosurfactants). *Current Opinion in Colloid & Interface Science*. 2002;**7**(1-2):12-20
- [31] D'aes J, De Maeyer K, Pauwelyn E, Höfte M. Biosurfactants in plant-Pseudomonas interactions and their importance to biocontrol: Biosurfactants in plant-Pseudomonas interactions. *Environmental Microbiology Reports*. 2009;**2**(3):359-372
- [32] Singh P, Cameotra SS. Potential applications of microbial surfactants in biomedical sciences. *Trends in Biotechnology*. 2004;**22**(3):142-146
- [33] Mulligan CN. Recent advances in the environmental applications

of biosurfactants. *Current Opinion in Colloid & Interface Science*. 2009;**14**(5):372-378

[34] Sachdev DP, Cameotra SS. Biosurfactants in agriculture. *Applied Microbiology and Biotechnology*. 2013;**97**(3):1005-1016

[35] Singh A, Van Hamme JD, Ward OP. Surfactants in microbiology and biotechnology: Part 2. Application aspects. *Biotechnology Advances*. 2007;**25**(1):99-121

[36] Reasoner DJ, Geldreich EE. A new medium for the enumeration and subculture of bacteria from potable water. *Applied Environmental Microbiology*. 1985;**49**:7

[37] Reiling HE, Thanei-Wyss U, Guerra-Santos LH, Hirt R, Käppeli O, Fiechter A. Pilot plant production of rhamnolipid biosurfactant by *Pseudomonas aeruginosa*. *Applied and Environmental Microbiology*. 1986;**51**(5):985

[38] Haba E, Pinazo A, Jauregui O, Espuny MJ, Infante MR, Manresa A. Physicochemical characterization and antimicrobial properties of rhamnolipids produced by *Pseudomonas aeruginosa* 47T2 NCBIM 40044. *Biotechnology and Bioengineering*. 2003;**81**(3):316-322

[39] Hansen FK, Rødsrud G. Surface tension by pendant drop. *Journal of Colloid and Interface Science*. 1991;**141**(1):1-9

[40] Smyth TJP, Perfumo A, McClean S, Marchant R, Banat IM. Isolation and analysis of lipopeptides and high molecular weight biosurfactants. In: Timmis KN, éditeur. *Handbook of Hydrocarbon and Lipid Microbiology*. Berlin, Heidelberg: Springer Berlin Heidelberg; 2010. pp. 3687-3704.

Disponible sur: [http://link.springer.com/10.1007/978-3-540-77587-4\\_290](http://link.springer.com/10.1007/978-3-540-77587-4_290)

[41] Gerard J, Lloyd R, Barsby T, Haden P, Kelly MT, Andersen RJ, et al. Antimycobacterial cyclic depsipeptides produced by two pseudomonads isolated from marine habitats. *Journal of Natural Products*. 1997;**60**(3):223-229

[42] Saini HS, Barragán-Huerta BE, Lebrón-Paler A, Pemberton JE, Vázquez RR, Burns AM, et al. Efficient purification of the biosurfactant viscosin from *Pseudomonas libanensis* strain M9-3 and its physicochemical and biological properties. *Journal of Natural Products*. 2008;**71**(6):1011-1015

[43] Braun PG, Hildebrand PD, Ells TC, Kobayashi DY. Evidence and characterization of a gene cluster required for the production of viscosin, a lipopeptide biosurfactant, by a strain of *Pseudomonas fluorescens*. *Canadian Journal of Microbiology*. 2001;**47**(4):294-301

[44] de Bruijn I, de Kock MJD, Yang M, de Waard P, van Beek TA, Raaijmakers JM. Genome-based discovery, structure prediction and functional analysis of cyclic lipopeptide antibiotics in *Pseudomonas* species. *Molecular Microbiology*. 2007;**63**(2):417-428

[45] Roongsawang N, Washio K, Morikawa M. Diversity of nonribosomal peptide synthetases involved in the biosynthesis of lipopeptide biosurfactants. *International Journal of Molecular Sciences*. 2011;**12**(1):141-172

[46] de Bruijn I, de Kock MJD, de Waard P, van Beek TA, Raaijmakers JM. Massetolide A biosynthesis in *Pseudomonas fluorescens*. *Journal of Bacteriology*. 2008;**190**(8):2777

[47] Berti AD, Greve NJ, Christensen QH, Thomas MG. Identification of a biosynthetic gene cluster and the six associated lipopeptides involved in

- swarming motility of *Pseudomonas syringae* pv. tomato DC3000. *Journal of Bacteriology*. 2007;**189**(17):6312
- [48] Burch AY, Zeisler V, Yokota K, Schreiber L, Lindow SE. The hygroscopic biosurfactant syringafactin produced by *Pseudomonas syringae* enhances fitness on leaf surfaces during fluctuating humidity. *Environmental Microbiology*. 2014;**16**(7):2086-2098
- [49] Marrink SJ, Risselada HJ, Yefimov S, Tieleman DP, de Vries AH. The MARTINI force field: Coarse grained model for biomolecular simulations. *The Journal of Physical Chemistry. B*. 2007;**111**(27):7812-7824
- [50] Marrink SJ, de Vries AH, Mark AE. Coarse grained model for semiquantitative lipid simulations. *The Journal of Physical Chemistry. B*. 2004;**108**(2):750-760
- [51] Ndao M, Goujon F, Ghoufi A, Malfreyt P. Coarse-grained modeling of the oil–water–surfactant interface through the local definition of the pressure tensor and interfacial tension. *Theoretical Chemistry Accounts*. 2017;**136**(1):21
- [52] Ndao M, Devémy J, Ghoufi A, Malfreyt P. Coarse-graining the liquid–liquid interfaces with the MARTINI force field: How is the interfacial tension reproduced? *Journal of Chemical Theory and Computation*. 2015;**11**(8):3818-3828
- [53] Goujon F, Dequidt A, Ghoufi A, Malfreyt P. How does the surface tension depend on the surface area with coarse-grained models? *Journal of Chemical Theory and Computation*. 2018;**14**(5):2644-2651
- [54] Ghoufi A, Goujon F, Lachet V, Malfreyt P. Multiple histogram reweighting method for the surface tension calculation. *The Journal of Chemical Physics*. 2008;**128**(15):154718
- [55] Ghoufi A, Malfreyt P, Tildesley DJ. Computer modelling of the surface tension of the gas–liquid and liquid–liquid interface. *Chemical Society Reviews*. 2016;**45**(5):1387-1409
- [56] Paredes X, Fernández J, Pádua AAH, Malfreyt P, Malberg F, Kirchner B, et al. Bulk and liquid–vapor interface of pyrrolidinium-based ionic liquids: A molecular simulation study. *The Journal of Physical Chemistry. B*. 2014;**118**(3):731-742
- [57] Ghoufi A, Malfreyt P. Entropy and enthalpy calculations from perturbation and integration thermodynamics methods using molecular dynamics simulations: Applications to the calculation of hydration and association thermodynamic properties. *Molecular Physics*. 2006;**104**(18):2929-2943
- [58] Ghoufi A, Emile J, Malfreyt P. Recent advances in many body dissipative particles dynamics simulations of liquid-vapor interfaces. *European Physical Journal E: Soft Matter and Biological Physics*. 2013;**36**(1):10
- [59] Maurel G, Schnell B, Goujon F, Couty M, Malfreyt P. Multiscale modeling approach toward the prediction of viscoelastic properties of polymers. *Journal of Chemical Theory and Computation*. 2012;**8**(11):4570-4579
- [60] Goujon F, Malfreyt P, Tildesley DJ. Interactions between polymer brushes and a polymer solution: Mesoscale modelling of the structural and frictional properties. *Soft Matter*. 2010;**6**(15):3472-3481